AD 400 514

63-3-J

FTD-TT- 62-1738

TRANSLATION

HEAT POWER ENGINEERING
(SELECTED ARTICLES)

FOREIGN TECHNOLOGY DIVISION

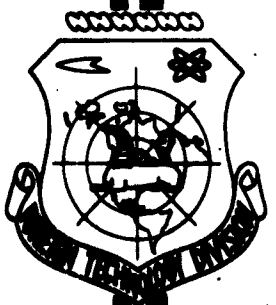

AIR FORCE SYSTEMS COMMAND

WRIGHT-PATTERSON AIR FORCE BASE

OHIO

UNEDITED ROUGH DRAFT TRANSLATION

HEAT POWER ENGINEERING (SELECTED ARTICLES)

English Pages: 40

SOURCE: Russian Periodical, Teploenergetika, Nr. 6
1962, pp. 24-31, 88-91, 92-93

SOV/96-62-0-6-4/11
SOV/96-62-0-6
SOV/96-62-0-6-11/11

PREPARED BY:

TRANSLATION SERVICES BRANCH
FOREIGN TECHNOLOGY DIVISION
WP-AFB, OHIO.

TABLE OF CONTENTS

AN APPROXIMATE SOLUTION TO A TWO-DIMENSIONAL STATIONARY HEAT-CONDUCTION PROBLEM AND ITS USE IN THE DETERMINATION OF THE EFFECT OF ARTIFICIAL COOLING OF TURBINE COMPONENTS

D. A. Pereverzev, Eng.

Hydraulic Machine Laboratory, Acad. Sci. Ukr. SSR.

Certain generalized solutions to the problem of a stationary temperature field in a semibounded body with internal cylindrical heat sources and approximate solutions to problems with boundary conditions of the third type are given. The equations derived were used to calculate the effect of cooling a turbine drum rotor.

Let us consider the problem of a stationary temperature field in a semibounded body with internal cylindrical heat sources.

Let there be distributed within the semibounded body at one and the same depth $\underline{h}$, but with different distances between their axes ($2x_1$ and S; $x_1 < S/4$), an infinite series of cylindrical channels of diameter $d = 2r$ (Fig. 1). The surface temperatures of the body t_Γ and the cylindrical channels t_o (boundary conditions of the first type) are given, with $t_\Gamma > t_o$ (cooling of the body by a system of submerged channels. The heat flux $\underline{q}$ issuing from a unit length of the channel and the heat-conduction coefficient of the body λ are assumed to be

constant. We shall assume that the axes of the channels are parallel to the surface of the body. With these stipulations, the process of heat propagation for a stationary state is described by the differential equation of heat conduction:

$$\frac{\partial^2 t(x,y)}{\partial x^2}+\frac{\partial^2 t(x,y)}{\partial y^2}=0. \qquad (1)$$

The x-axis is located on the surface of the body, while the y-axis is symmetrical with respect to adjacent channels (Fig. 1). It is necessary to find a solution to Eq. (1) which satisfies the given boundary conditions (t_r and t_0).

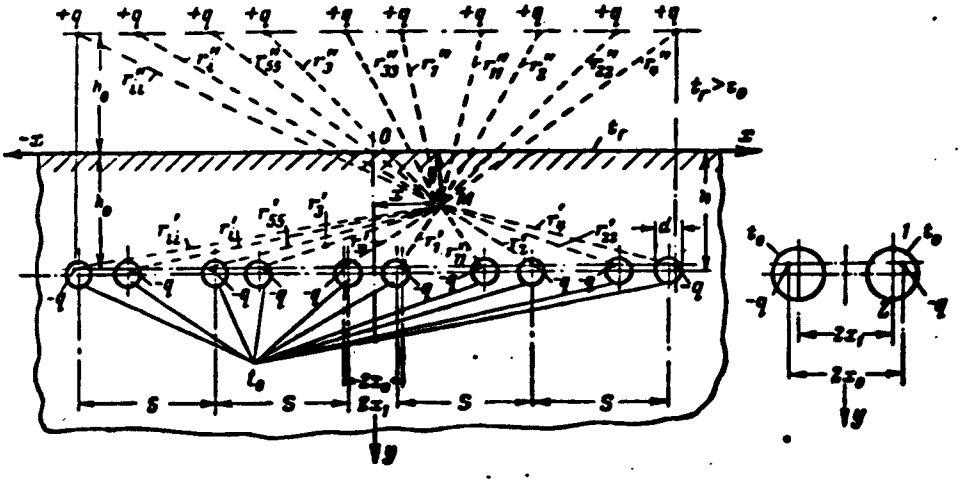

Fig. 1. Schematic for the derivation of the temperature-field equation.

We shall use the method of superposition, in order to solve Eq. (1). We shall assume that the thermal capacity of the first channel is concentrated along a line having the coordinates $x = x_0$, $y = h_0$ and parallel to the axis of the channel. By analogy, taking the condition of symmetry into account, we do the same thing with the remaining channels. We obtain a system of point sinks (-q). Symmetri-

cal with them we set up a system of sources of the same capacity (+q). The temperature t at an arbitrary point M(x, y) is determined from the superposition of the temperature fields produced by the system of point sources and sinks.

We introduce the notation $\theta = t_\Gamma - t$. Then the temperature field of a sink is determined from the expression:

$$\theta' = \frac{q}{2\pi\lambda} \ln \frac{h_0}{r'},$$

and the temperature field of a source by the dependence

$$\theta'' = \frac{q}{2\pi\lambda} \ln \frac{r''}{h_0}.$$

The total effect of the source and the sink gives the temperature field:

$$\theta'' = \theta' + \theta'' = \frac{q}{2\pi\lambda} \ln \frac{r''}{r'}.$$

As a result of the combined effect of all sources and sinks (Fig. 1), we obtain the temperature field:

$$\theta = t_\Gamma - t = \frac{q}{2\pi\lambda}\left(\ln \frac{r_1''}{r_1'} + \ln \frac{r_{11}''}{r_{11}'} + \ln \frac{r_2''}{r_2'} + \right.$$
$$\left. + \ln \frac{r_{22}''}{r_{22}'} + \ldots + \ln \frac{r_i''}{r_i'} + \ln \frac{r_{ii}''}{r_{ii}'} + \ldots\right). \qquad (2)$$

Determining the values of the radii from geometrical considerations, (Fig. 1) and substituting in (2), we obtain, after transformations:

$$t_\Gamma - t = \frac{q}{4\pi\lambda}\left\{\left[\sum_{n=1}^{\infty} \ln \frac{[S\cdot n + (x - x_0)]^2 + (h_0 + y)^2}{[S\cdot n + (x - x_0)]^2 + (h_0 - y)^2} + \right.\right.$$
$$\left. + \sum_{n=0}^{\infty} \ln \frac{[S\cdot n - (x - x_0)]^2 + (h_0 + y)^2}{[S\cdot n - (x - x_0)]^2 + (h_0 - y)^2}\right] +$$
$$+ \left[\sum_{n=1}^{\infty} \ln \frac{[S\cdot n + (x + x_0)]^2 + (h_0 + y)^2}{[S\cdot n + (x + x_0)]^2 + (h_0 - y)^2} + \right.$$
$$\left.\left. + \sum_{n=1}^{\infty} \ln \frac{[S\cdot n - (x + x_0)]^2 + (h_0 + y)^2}{[S\cdot n - (x + x_0)]^2 + (h_0 - y)^2}\right]\right\}. \qquad (3)$$

Here the first bracket includes channels with subscripts i, while the second bracket includes channels with subscripts ii to the right and left of the y-axis, respectively, (Fig. 1).

According to page 282 of Ref. [1], we have

$$* \quad \frac{\operatorname{ch} u - \cos V}{2 \sin^2 \frac{V}{2}} = \left(1 + \frac{u^2}{V^2}\right) \prod_{k=1}^{\infty} \left[1 + \frac{u^2}{(2k\pi + V)^2}\right] \times$$

$$\times \left[1 + \frac{u^2}{(2k\pi - V)^2}\right].$$

Expression (3) is easily reduced to this form by the substitution:

$$h_0 + y = \frac{S}{2\pi} u_1; \; h_0 - y = \frac{S}{2\pi} u_2; \; x - x_0 = \frac{S}{2\pi} V_1;$$

$$x + x_0 = \frac{S}{2\pi} V_2.$$

We shall convert the series in the brackets of equality (3) into infinite products. After substitution and transformations we obtain:

for the first bracket

$$\ln \left\{ \frac{1 + \frac{u_1^2}{V_1^2}}{1 + \frac{u_2^2}{V_1^2}} \prod_{n=1}^{\infty} \frac{\left[1 + \frac{u_1^2}{(2n\pi + V_1)^2}\right]\left[1 + \frac{u_1^2}{(2n\pi - V_1)^2}\right]}{\left[1 + \frac{u_2^2}{(2n\pi + V_1)^2}\right]\left[1 + \frac{u_2^2}{(2n\pi - V_1)^2}\right]} \right\} =$$

$$= \ln \frac{\operatorname{ch} u_1 - \cos V_1}{\operatorname{ch} u_2 - \cos V_1} =$$

$$= \ln \frac{\operatorname{ch} \frac{2\pi}{S}(h_0 + y) - \cos \frac{2\pi}{S}(x - x_0)}{\operatorname{ch} \frac{2\pi}{S}(h_0 - y) - \cos \frac{2\pi}{S}(x - x_0)}; \qquad (3a)$$

analogously for the second bracket

$$\ln \frac{\operatorname{ch} \frac{2\pi}{S}(h_0 + y) - \cos \frac{2\pi}{S}(x + x_0)}{\operatorname{ch} \frac{2\pi}{S}(h_0 - y) - \cos \frac{2\pi}{S}(x + x_0)}. \qquad (3b)$$

The heat flux issuing from a unit length of the channel is:

$$q = \frac{2\pi\lambda(t_1 - t_0)}{k_0}. \qquad (3c)$$

---

* ch = cosh

where R_0 is the dimensionless thermal resistance of the channel.

Substituting (3a), (3b), and (3c) into (3) we obtain, after simple transformations

$$\bar{\tau}=\frac{t-t_0}{t_c-t_0}=1-$$
$$-\frac{1}{2R_0}\ln\left[\frac{\operatorname{ch}\frac{2\pi}{S}(h_0+y)-\cos\frac{2\pi}{S}(x-x_0)}{\operatorname{ch}\frac{2\pi}{S}(h_0-y)-\cos\frac{2\pi}{S}(x-x_0)}\times\right.$$
$$\left.\times\frac{\operatorname{ch}\frac{2\pi}{S}(h_0+y)-\cos\frac{2\pi}{S}(x+x_0)}{\operatorname{ch}\frac{2\pi}{S}(h_0-y)-\cos\frac{2\pi}{S}(x+x_0)}\right]. \tag{4}$$

where $\bar{\tau}$ is the relative excess temperature at the point of the body under consideration.

The value of $\underline{t}$ determined from (4) satisfies equation (4) and a boundary condition of the first type on the surface of the body (for $y = 0$, $\bar{\tau} = 1$, or $t = t_T$).

It can be shown that for $x_0 = 0$ and $x_0 = S/4$, the equality (4) leads to the solutions obtained in Refs. [2 and 3] for equally distributed channels.

In order to satisfy the boundary condition $\bar{\tau} = 0$ ($t = t_0$) over the entire contour of the channel, we have at our disposal in Eq. (4) only three constants: x_0, h_0, and R_0. With their aid the condition $\bar{\tau} = 0$ may be satisfied at only three arbitrary points of the original contour. The remaining points of the isotherm $\bar{\tau} = 0$ are determined from the equation

$$\frac{\operatorname{ch}\frac{2\pi}{S}(h_0+y)-\cos\frac{2\pi}{S}(x-x_0)}{\operatorname{ch}\frac{2\pi}{S}(h_0-y)-\cos\frac{2\pi}{S}(x-x_0)}\times$$
$$\times\frac{\operatorname{ch}\frac{2\pi}{S}(h_0+y)-\cos\frac{2\pi}{S}(x+x_0)}{\operatorname{ch}\frac{2\pi}{S}(h_0-y)-\cos\frac{2\pi}{S}(x+x_0)}=e^{2R_0}. \tag{5}$$

which, in the general case, is not an equation of a circle.

Therefore Eq. (4) solves the given problem approximately. The approximateness is due to the fact that the thermal capacity of a circular cooling contour is concentrated in one discharge. The same thing applies to the solutions obtained in Refs. [2 and 3].

Thus, Eq. (4) is an exact solution of the problem for the contour described by Eq. (5), which, however, given a proper choice of the determining points and given small ratios r/S, may turn out to be very close to a circle. Calculations indicate that if the abscissa of a sink is given, assuming that $x_0 = x_1$, while points 1 and 2, located on the vertical diameter of the original contour (Fig. 1) are taken as the determining points, then such a choice ensures, for $r/S \leq 0.06$--0.07 over the entire possible range, a variation of h/S ($h > r$) and x_1/s ($r \leq x_1 \leq S/4$) and an almost complete coincidence between a circular contour and the contour described by Eq. (5).

Taking into account what has been said, let us determine the sink parameters in Eq. (4). Substituting the coordinates of the determining points 1 and 2 (Fig. 1) and taking into account the properties of hyperbolic functions, we obtain the following system of two equations with two unknowns (h_0 and R_0):

$$\text{point } 1\ x=x_1,\ y=h-r,\ \bar{l}=0$$

$$\ln\left\{\left[\frac{\operatorname{sh}^2\frac{\pi}{S}(h_0+h-r)}{\operatorname{sh}\frac{\pi}{S}(h_0-h+r)}\right]^2\frac{\operatorname{ch}\frac{2\pi}{S}(h_0+h-r)-\cos\frac{4\pi}{S}x_1}{\operatorname{ch}\frac{2\pi}{S}(h_0-h+r)-\cos\frac{4\pi}{S}x_1}\right\}= \tag{6}$$

$$=2R_0;$$

$$\text{point } 2\ x=x_1,\ y=h+r,\ \bar{l}=0$$

$$\ln\left\{\left[\frac{\operatorname{sh}\frac{\pi}{S}(h_0+h+r)}{\operatorname{sh}\frac{\pi}{S}(h+r-h_0)}\right]^2\frac{\operatorname{ch}\frac{2\pi}{S}(h_0+h+r)-\cos\frac{4\pi}{S}x_1}{\operatorname{ch}\frac{2\pi}{S}(h+r-h_0)-\cos\frac{4\pi}{S}x_1}\right\}=$$

$$=2R_0.$$

* sh = sinh (7)

An analytical solution of the system of equations (6), (7) in general form is impossible. But with $x_1 = 0$ and $x_1 = S/4$, the system is simplified. Equating (6) and (7) and applying the formulas of hyperbolic trigonometry, after transformations, we have:

1. With $x_1 = 0$

$$\operatorname{ch}\frac{2\pi}{S}h_0 = \frac{\operatorname{ch}\frac{2\pi}{S}h}{\operatorname{ch}\frac{2\pi}{S}r},$$

or

$$\frac{2\pi}{S}h_0 = \ln\left[\frac{\operatorname{ch}\frac{2\pi}{S}h}{\operatorname{ch}\frac{2\pi}{S}r} \pm \sqrt{\frac{\operatorname{ch}^2\frac{2\pi}{S}h}{\operatorname{ch}^2\frac{2\pi}{S}r} - 1}\right] =$$

$$= \pm\ln\left[\frac{\operatorname{ch}\frac{2\pi}{S}h}{\operatorname{ch}\frac{2\pi}{S}r} + \sqrt{\frac{\operatorname{ch}^2\frac{2\pi}{S}h}{\operatorname{ch}^2\frac{2\pi}{S}r} - 1}\right].$$

Here the positive root gives the ordinate of the sink, while the negative root give the ordinate of the source. We are interested only in the values $y > 0$. Therefore, we assume finally that:

$$\frac{2\pi}{S}h_0 = \ln\left[\frac{\operatorname{ch}\frac{2\pi}{S}h}{\operatorname{ch}\frac{2\pi}{S}r} + \sqrt{\frac{\operatorname{ch}^2\frac{2\pi}{S}h}{\operatorname{ch}^2\frac{2\pi}{S}r} - 1}\right]. \tag{8}$$

Substituting (8) in (6) or (7), we obtain:

$$R_0 = \ln\left[\frac{\operatorname{sh}\frac{2\pi}{S}h}{\operatorname{sh}\frac{2\pi}{S}r} + \sqrt{\frac{\operatorname{sh}^2\frac{2\pi}{S}h}{\operatorname{sh}^2\frac{2\pi}{S}r} - 1}\right]. \tag{9}$$

2. With $x_1 = S/4$

$$\frac{4\pi}{S}h_0 = \ln\left[\frac{\operatorname{ch}\frac{4\pi}{S}h}{\operatorname{ch}\frac{4\pi}{S}r} + \sqrt{\frac{\operatorname{ch}^2\frac{4\pi}{S}h}{\operatorname{ch}^2\frac{4\pi}{S}r} - 1}\right]. \tag{10}$$

$$R_0 = \ln\left[\frac{\operatorname{sh}\frac{4\pi}{S}h}{\operatorname{sh}\frac{4\pi}{S}r} + \sqrt{\frac{\operatorname{sh}^2\frac{4\pi}{S}h}{\operatorname{sh}^2\frac{4\pi}{S}r} - 1}\right]. \tag{11}$$

For $0 < x_1 < S/4$, h_o lies between the values determined according to (8) and (10). This makes possible a relatively simple solution of Eqs. (6) and (7) in numerical form by selection of the quantity h_o. For practical calculations, h_o may be determined adequately enough from (10). Moreover, the quantities R_o, calculated according to (6) and (7), turn out to be sufficiently close to each other. If they are different, then to increase the accuracy of the subsequent calculations of temperature according to Eq. (4), it is necessary to introduce their average value.

If $\underline{r}$ is substantially less than $\underline{h}$ and S, then it is possible to set $h_o = h$, $\sinh \pi/S\ r = \frac{\pi}{S} r$, $\cosh \frac{2\pi}{S} r = 1$, while from expression (6) or (7) we obtain:

$$R_o = \frac{1}{2} \ln \left[\left(\frac{\operatorname{sh} \frac{2\pi}{S} h}{\frac{\pi}{S} r} \right)^2 \frac{\operatorname{ch} \frac{4\pi}{S} h - \cos \frac{4\pi}{S} x_1}{1 - \cos \frac{4\pi}{S} x_1} \right]. \qquad (12)$$

The degree of accuracy of the solution may be increased, if it is constructed with the aid of several heat sinks. Let the number of sinks be equal to $\underline{m}$. In this case there will be $3m$ constants which make it possible to satisfy the boundary condition $\bar{t} = 0$ at $3m$ points of the given circle. It is possible by such a method to obtain a solution of the problem for channels with contours of arbitrary shape.

Applying the method of superposition for an arbitrary point M (Fig. 2), we obtain in this case:

$$t_r - t = \sum_{i=1}^{m} \frac{q_i}{4\pi\lambda} \ln \frac{\operatorname{ch} \frac{2\pi}{S} (h_{oi} + y) - \cos \frac{2\pi}{S} (x - x_{oi})}{\operatorname{ch} \frac{2\pi}{S} (h_{oi} - y) - \cos \frac{2\pi}{S} (x - x_{oi})} \qquad (13)$$

or in relative units

$$\bar{t} = \frac{t - t_o}{t_r - t_o} = 1 - \\ - \sum_{i=1}^{m} \frac{1}{2R_{oi}} \ln \frac{\operatorname{ch} \frac{2\pi}{S} (h_{oi} + y) - \cos \frac{2\pi}{S} (x - x_{oi})}{\operatorname{ch} \frac{2\pi}{S} (h_{oi} - y) - \cos \frac{2\pi}{S} (x - x_{oi})}, \qquad (14)$$

where m, x_{oi}, h_{oi} and R_{oi} are, respectively, the number, coordinates, and dimensionless thermal resistances of the sinks in the contour; S is the spacing of sinks of equal depth along the x-axis; $q_i = \frac{2\pi\lambda(t_r - t_0)}{R_{oi}}$ is the productivity of the sinks.

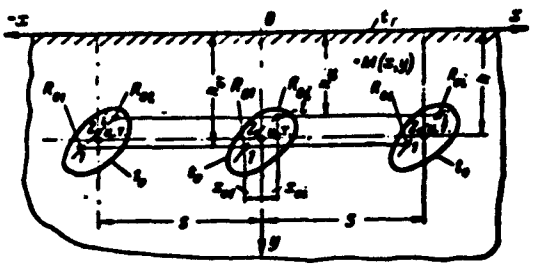

Fig. 2. Cooling of a semibounded body by a system of channels with contours of arbitrary shape.

The total thermal resistance of a channel with a contour of arbitrary shape is:

$$R = \frac{1}{2\pi\lambda \sum_{i=1}^{m} \frac{1}{R_{oi}}}. \qquad (15)$$

Here the y-axis is directed through the center of gravity of the transverse cross section of the channel, but it may be directed arbitrarily. The argumentation is not changed by this.

In a more general case there may be several series of channels which differ in the shape of their contour and in their spacing. In this case additional sums will appear in Eq. (13).

Every sink is characterized in (14) by three parameters: x_{oi}, h_{oi} and R_{oi}, which are still unknown. In order to determine them, it is necessary to set up a system of 3m equations from the condition $\bar{t} = 0$ with respect to the individual points of the cooling contours.

Given the number of sinks, it is possible to include any desired number of points of the contour. Put in this way, the problem may be solved with any desired degree of accuracy necessary in practice. The difficulties of solution of complex systems of algebraic equations in the determination of 3m unknowns may be eliminated by the use of electronic computers. In solving the system, it is necessary to take into account that the heat sinks must be distributed within the region

encompassed by the original contour.

In a number of cases the solution of the system is simplified. Thus, for example, for symmetrical contours, the number of unknowns may be reduced by half. The number of unknowns may also be reduced, if the abscissas of several sinks are given. For circular contours, if r_i is significantly less than h_i and S_i, it is possible to set $h_{oi} = h_i$ (the sink coincides with the center of the circle), and then everything reduces to a solution of a system of linear algebraic equations with the unknowns $z_i = \frac{1}{R_{oi}}$.

Let us note some of the most important properties of the temperature field described by Eq. (14).

1. The temperature of a body at infinity is determined by the relationship

$$\bar{t}_{y=\infty} = \lim_{y \to \infty} \bar{t} = 1 - \sum_{i=1}^{n} \frac{\frac{2\pi}{S} h_{oi}}{R_{oi}}. \tag{16}$$

2. Let us consider, for any y below the cooling channels, the heat flux and the average temperature of the body in a step-type cross section. In the general case, their values are expressed by the relationships:

heat flux

$$Q = -\lambda (t_r - t) \int_0^S \frac{\partial \bar{t}}{\partial y} dx, \tag{17}$$

average temperature of the body

$$\bar{t}_0 = \frac{1}{S} \int_0^S \bar{t}\, dx. \tag{18}$$

Then

$$\frac{d\bar{t}_0}{dy} = \frac{1}{S} \int_0^S \frac{\partial \bar{t}}{\partial y} dx. \tag{18a}$$

But below the cooling channels for any y, $Q = 0$, and therefore

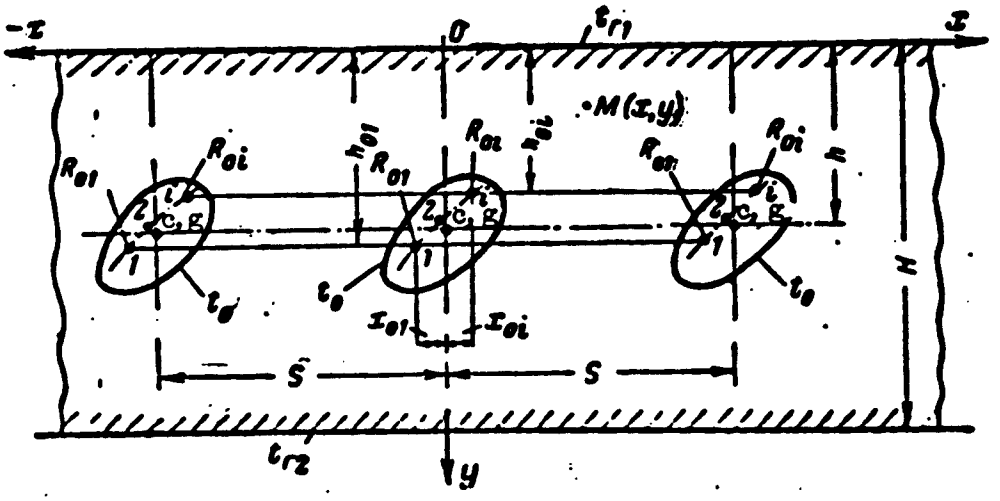

Fig. 3. Flat wall with internal cooling channels.

$\frac{d\bar{t}_c}{dy} = 0$, or $\bar{t}_c = \text{const} = \bar{t}_y = \infty$. With a reduction in y from the value y_1 (y_1 is the ordinate of the lower point of the deepest contour), $\bar{t}_c$ starts to increase. Consequently, below the cooling channels the average temperature of the object in a step-type cross section (designated by $\bar{t}_{c\ min}$ has a minimum value and is equal in all cross sections to the temperature at infinity.

3. The nonuniformity of the temperature with respect to the spacing decreases rapidly with increasing distance from the cooling channel into the interior of the body. Calculations indicate that at the relative depth $\frac{y}{S} \geq \frac{h_{01}}{S} + (0.4 - 0.5)$ (h_{01} is the ordinate of the lower sink) the temperature field at all points of the body is practically leveled to the temperature at infinity.

By virtue of the above-enumerated properties, the temperature $t_{y=\infty} = \bar{t}_{c\ min}$ may serve as a practical criterion of the effectiveness of cooling a semibounded body with a system of submerged channels. The relatively simple expression (16) significantly simplifies calculations in the choice of the optimum dimensions of the channels. This temperature may serve as a criterion for the most rational choice of the number of sinks. For example, if the furthest increase in the number of sinks does not alter essentially the quantity $t_{c\ min}$ then it may be assumed that a satisfactorily accurate solution has been attained.

A third property of the field makes it possible to solve (14) for the calculation of temperatures in flat walls with a thickness $\frac{H}{S} \geq \frac{h_{01}}{S} +$ (0.4-0.5), if the lower surface of the wall opposite the heat-supplying side is free from heat exchange.

If the temperatures of both surfaces of the wall t_{r1} and t_{r2} are given, where t_{r2} may be either larger or smaller than t_0, then with

$\frac{H}{S} \geq \frac{h_{OH}}{S} +$ (0.4-0.5) the equation of the temperature field may be expressed accurately enough in the form of a sum of particular solution:

$$t_{r1} - t = -\sum_{i=1}^{m} \frac{q_i}{4\pi\lambda} \ln \frac{\operatorname{ch} \frac{2\pi}{S}(h_{oi} + y) - \cos \frac{2\pi}{S}(x - x_{oi})}{\operatorname{ch} \frac{2\pi}{S}(h_{oi} - y) - \cos \frac{2\pi}{S}(x - x_{oi})} + Cy. \qquad (19)$$

The solution of (19) satisfies Eq. (1) and the boundary condition on the upper surface of the wall, when y = 0 and t = t_{r1}. To determine the sink parameters and the constant C, it is necessary to use the boundary conditions t = t_o along the cooling contour with y = H and t = t_{r2}. The latter condition, taking into account the first and third properties of the temperature field described by Eqs. (13) and (14), may be written thus:

for y = H

$$t_{r1} - t_{r2} = \sum_{i=1}^{m} \frac{q_i h_{oi}}{\lambda S} + CH. \qquad (20)$$

For a semibounded body and flat wall, a comparison was made of the circle and the curved isotherms t = t_o obtained from Eqs. (13) and (19) for m = 1 and x_o = 0 (equally submerged and equally distributed cooling channels). As can be seen from Fig. 4, the isotherm t = t_o, with a reduction in r/S, in both variations approximates a circle more and more. With r/S = 0.05, all three curves practically merge into one. On the whole, for r/S $\leq$ 0.1 the replacement of the thermal capacity of a circular channel with a single point heat sink ensures good accuracy of solution. Alternative calculations indicate that this holds true even for h/S < 0.5, provided that the condition h > r is observed. For h/S > 0.5 a good accuracy of solution may be obtained even for r/S > 0.1.

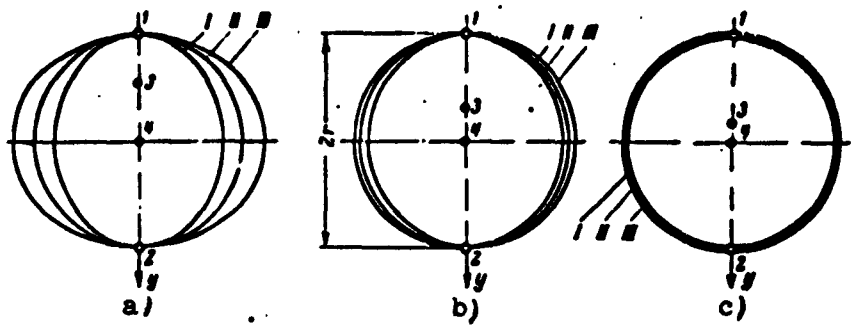

Fig. 4. Degree of approximation of the isotherm $t = t_0$ to a circular contour (equally submerged and equally distributed channels) in the presence of a single heat sink in the contour.

I) in a semibounded body; II) circle; III) in a flat wall ($H = 2h$, $t_{\Gamma 1} = t_{\Gamma 2} = t_\Gamma$).

1, 2) analogous to Fig. 1; 3, 4) location of point heat sinks in a semibounded body and a flat wall respectively. Initial data: $h/S = 0.5$; $H/S = 1$; a - $r/S = 0.2$; b - $r/S = 0.1$; c - $r/S = 0.05$.

In practice, we encounter more frequently boundary conditions of the third type, where the temperatures of the media adjacent to the heat-supplying (t_Γ) and heat-removing (t_0) surfaces are given.

Below is a proposed solution of such problems by the method of the additional wall. It consists of the following.

A layer of metal is added arbitrarily to the heat-supplying side

$$\Delta = \frac{\lambda}{\alpha_\Gamma} = \frac{S}{Bi_\Gamma}. \qquad (21)$$

The origin of the coordinates is raised by the amount Δ, and the depth of the channel must now be taken as $h_f = h + \Delta$. For a flat wall in the presence of boundary conditions of the third type, layers of metal are added to both surfaces of the wall:

$$\Delta_1 = \frac{\lambda}{\alpha_{\Gamma 1}}; \quad \Delta_2 = \frac{\lambda}{\alpha_{\Gamma 2}}.$$

An additional cylindrical layer is arbitrarily added to the heat-removing side. The inner diameter of this layer is determined by the relationship

$$\frac{2\pi\lambda(t_{II}-t_0)}{\ln\frac{d}{d_f}}=\pi d\alpha_0(t_{II}-t_0), \tag{22}$$

whence we obtain:

$$d_f=de^{-\frac{2\lambda}{\alpha_0 d}}=de^{-\frac{2}{Bi_0}}. \tag{23}$$

In formulas (21) and (23)

$$Bi_T=\frac{\alpha_T S}{\lambda};\ Bi_0=\frac{\alpha_0 d}{\lambda}$$

(the Biot criteria for the heat-supplying and heat-removing sides, respectively);

λ = the heat-conduction coefficient of the body determined from the average temperature of the body;

α_T and α_0 = the heat-transfer coefficients on the heat-supplying and heat-removing sides (taken as constants);

t_{II} = the average temperature of the surface of the cooling channel;

S = the spacing of the channels;

d = the diameter of the cooling channel;

d_f = the hypothetical diameter of the cooling channel (inner diameter of the additional cylindrical layer)

A channel with a contour of arbitrary shape may be replaced by a system of circular channels inscribed in it, provided that the total perimeter of the circular channels and the heat-transfer coefficient in them are kept equal to the original (u and α_0). In this case the hypothetical diameter is determined by the formula

$$d_f=d_{II}e^{-\frac{2}{\alpha_0 d_{II}}}=d_{II}e^{-\frac{2\lambda}{d_{II}\alpha_0}}, \tag{24}$$

where d_{II} = diameter of one of the circles replacing the original contour

$Bi_o = \frac{\alpha_o d_e}{\lambda}$ = Biot criterion on the heat-removing side

$d_e = \frac{4F}{u}$ = effective diameter of the original contour

α_o = heat-transfer coefficient in the original channel

In formulas (4) and (20), $\underline{h}$ and $\underline{d}$ are replaced by h_f and d_f, and the problem is thus reduced to a problem with boundary conditions of the first type. Consequently, for boundary conditions of the third type, $\bar{\tau}$ no longer depends only on geometrical factors, but also on the magnitudes of Bi_T and Bi_o.

Analysis of alternative calculations shows that with the substitutions indicated, a small variation in the thermal resistance of the body itself occurs. This is expressed in a certain deformation (as compared with the real picture) of the temperature field near the original channel, which, for all practical purposes, has little effect on the accuracy of the calculations. With an increase in the external resistances (with a reduction of α_T and especially α_o) the influence of these errors decreases, and the accuracy of the calculations increases. The same thing takes place with an increase in the depth of the channels. Thus, even with $h/S > 0.5$ a contour of arbitrary shape may be replaced by a single circular one at the same depth $\underline{h}$ without great loss of accuracy in the solution (the determination of the cooling effect).

Since there is no strict solution to the problem, the limits of applicability of the method of the additional wall can be established only through comparison with experiments and with other more accurate methods of calculation (e.g., the ETA method).

The solutions derived were used in the calculation of the cooling effect in a drum rotor of a steam turbine.

Figure 5 shows an element of the cooled drum rotor of the SKR-100 KhTGZ turbine designed for the initial steam parameters of 300 atm (abs)

and 650° C. Cooling is accomplished by a stream of steam of reduced temperature (525° C) flowing along specially provided channels in the tails of working blades 1 and in intermediate inserts 2, which shield the surface of the rotor in the zone of distribution of guide vanes 3 [4, 5]. A section of an element indicated by dot-dash lines and solid shading was studied by the ETA method on solid and plane models in electrolytic baths [5].*

For the solid model it was assumed that the drum rotor was made of perlitic steel, and the blades and inserts of austenitic steel. For the plane model (semibounded body) the heat-conduction coefficient λ was taken equal to the heat-conduction coefficient of the material of the austenitic blades. The depth, the dimensions and also α_o of the slit in the plane model were taken the same as for the working blades in the solid model. The spacing was taken equal to the root spacing of the working blades.

Figures 5a and 5b give the temperature fields obtained on solid and plane models for nominal working conditions on a section of the second reactive stage. Comparison of them shows that below the cooling channels the temperature of both models levels off rapidly, while the average temperature ($\bar{t}_{c\ min}$) on the plane model is only 0.01-0.2 higher than the temperature of the rotor (0.173 as against 0.15-0.16 This makes it possible, in the given case, to substitute a plane problem for a solid one and to consider the temperature of the rotor as the temperature of a semibounded body at infinity.

---

* It was assumed that on the boundaries of an isolated element axial temperature gradients do not exist. Experiments [5] have shown that the temperature of the rotor drum varies insignificantly from stage to stage (it decreases with the flow rate of the steam), so that this assumption was justified.

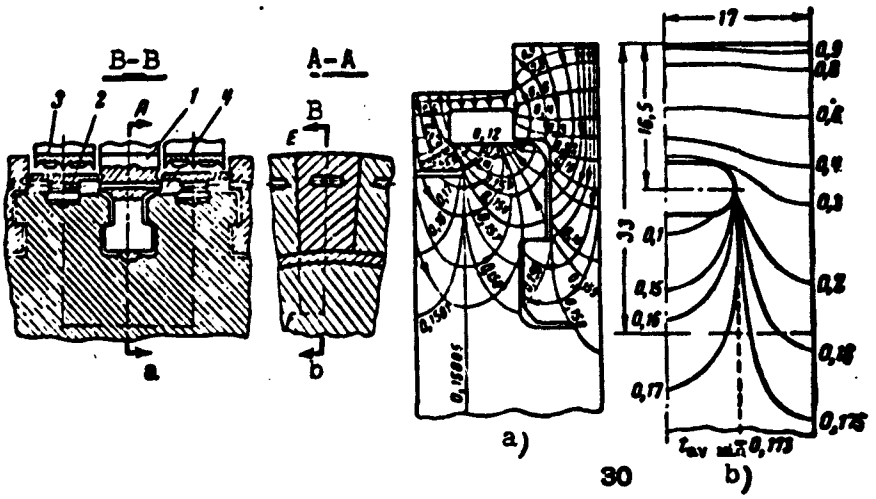

Fig. 5. Element of a cooled rotor studied by the ETA method.

a) temperature field in the cross section EF obtained on the solid model; cooling channels; in the blade) plane slit 6 x 16 mm; in the insert) circular channel with 3 mm diameter; b) temperature field obtained on the plane model, Bi_Γ/Bi_o = 19.15/2.25; cooling channel) plane slit 6 x 16 mm.

In accordance with (6), (10), and (16), relative temperatures were calculated for the nominal and certain variable regimes. The plane slit was replaced by two circular channels while keeping the original $\underline{u}$ and α_o. The basic geometrical dimensions of the slit and the results of the calculation are presented in the table. Also presented in the table are ETA data, which were obtained for analogous Bi_Γ and Bi_o at the Department of Turbine Construction of the Kharkov Polytechnical Institute by V. M. Kapinos and Ye. I. Bublikov. The results of the calculations and the ETA data coincide almost completely.

It should be emphasized that the plane model under consideration takes into account well enough complex heat exchange at the root of the blades and in the transition chamber 4 (Fig. 5) for the actual

case which was investigated in the literature [5]. However, it is not impossible that for other geometries of the cooling channels and other boundary conditions, the heat-transfer results obtained on plane and solid models will differ more significantly.

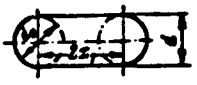

	M_0	0.5	0.75	1	1.25	1.5	1.75	2	2.2	M_T
$\bar{t}_p$	ETA estimate	0.465 0.460	0.368 0.370	0.305 0.309	0.262 0.263	0.233 0.229	0.207 0.205	0.190 0.185	0.178 0.174	} 10.83
$\bar{t}_p$	ETA estimate	0.449 0.444	0.355 0.352	0.292 0.296	0.249 0.251	0.220 0.218	0.195 0.195	0.178 0.176	0.164 0.166	} 11.15
$\bar{t}_p$	ETA estimate	0.422 0.420	0.327 0.325	0.268 0.270	0.227 0.229	0.203 0.199	0.179 0.178	0.163 0.160	0.152 0.150	} 6.30

Nevertheless, the computational method proposed may be recommended for the selection of the optimum dimensions of cooling channels and for estimations of the temperature of a cooled drum rotor in designing new high-temperature turbines, if a system of cooling analogous to the one under consideration is used.

The solutions obtained may also be used for calculating the temperature of disks cooled by passing an appropriate medium through the flow areas of the tail sections of the blades or immediately on the rim of the disk (assembly clearances, borings, etc.). Moreover, if there is an absence of additional heat removal from the web of the disk, then solutions of type (4) and (14) are applicable. In the presence of additional heat removal from the web of the disk, the equations of the temperature field may be obtained by "stitching together" solution (19) and the widely known solution of the one-dimensional problem for a disk [6]. The first of them will give the temperature distribution in the zone of the rim, the second will give the temperature distribution over the web of the disk.

Finally, Eqs. (14) and (19) permit determination of the thermal resistances of the channels (or tubes) with a complex cross-sectional profile, if these channels are laid in a semibounded body or a plane wall.

REFERENCES

1. I. M. Ryzhik. Tables of Integrals, Sums, Series and Products, Gostekhizdat, 1948.

2. I. A. Ioffe, ZhTF, No. 5, 1958.

3. A. A. Sander. Izv. Vysshikh Uchebnykh Zavedeniy, "Stroitel'stvo i Arkhitektura", No. 1, 1958.

4. L. A. Shubenko-Shubin. "Teploenergetika", No. 2, 1960.

5. Ye. I. Bublikov and V. M. Kapinos, "Energomashinostroyeniye", No. 4, 1960.

6. I. T. Shvets and Ye. P. Dyban. Air Cooling of Gas-Turbine Rotors, Izd. Kievskovo Universiteta, 1959.

OPTIMUM DIFFUSER SHAPE

I. Ye. Virozub and A. Sh. Dorfman

It is well known that the basic type of loss in diffusers is expansion losses. For the case where the diffuser has straight-line generatrices (flat and conical) and the fluid is incompressible, expansion losses are usually determined by shock softening factor φ [1-3]. The essence of this method of determining losses is that expansion losses are equated with shock losses Δ_{sh}, determined by the Borda-Carnot theorem:

$$\Delta_{sh} = \frac{\rho}{2}(w_1 - w_e)^2. \qquad (1)$$

where ρ is the density; w_1 and w_e, stream velocities on intake and exit.

It is considered that expansion losses in diffusers with rectilinear generatrices make up part of the shock losses:

$$\Delta_{exp} = \varphi \Delta_{sh}. \qquad (2)$$

Many experiments (at least for an incompressible fluid) have ascertained that factor φ in Eq. 2 chiefly depends on the diffuser's expansion angle θ. Figure 1 shows the relationship $\varphi(\theta)$.

No doubts arise that the magnitude of the losses in the diffuser

in its prescribed length and degree of expansion will depend only on the shape of the walls forming this diffuser. Therefore the question comes up as to the selection of the medium for all diffusers of a prescribed length and degree of expansion, the expansion being such that losses in it are the least. This problem has attracted the attention of many researchers. In Idel'chik [2], for example, there is a survey of research on determining diffuser losses; and diffusers with straight-line and curvilinear generatrices are compared, as well as diffusers with abrupt changes in cross-sectional area. But the problem of choosing the diffuser shape in which losses are minimum is not posed in this research.

Formula (2) must not be directly used in computing a diffuser with curvilinear generatrices. Therefore in the following, when solving the problem of optimum diffuser shape, we use the concept of local expansion angle introduced in Dorfman et al. [4]:

$$\theta = 2\arctan\left(\frac{1}{U}\frac{dF}{dx}\right),$$

where F is the area of the longitudinal cross-section; U, the wet perimeter; and x, the longitudinal coordinate.

It is easy to show that for an axisymmetrical diffuser the foregoing expression leads to the form:

$$\tan\frac{\theta}{2} = \frac{dR}{dx}. \qquad (3)$$

where R is the radius of the cross-section of the diffuser.

We will examine an axisymmetrical diffuser of prescribed length and degree of expansion (Fig. 2). The shape of its generatrices must be determined from the condition that expansion losses have a minimum. The fundamental region of a diffuser of length dx may be seen isolated in Fig. 2 regarded as a conical diffuser with its

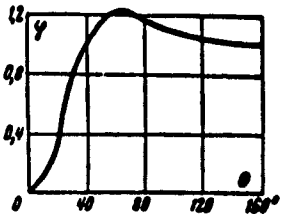

Fig. 1.

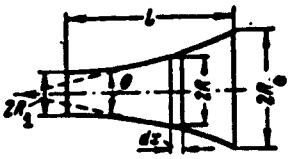

Fig. 2.

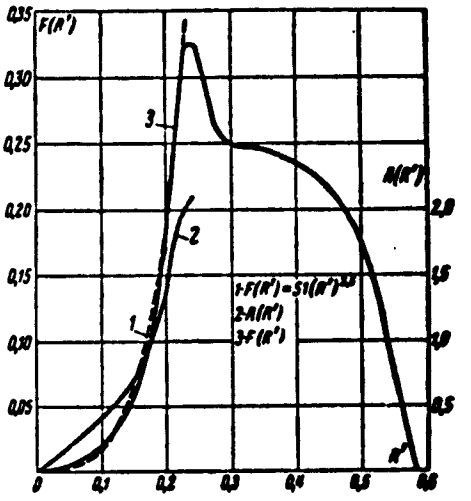

Fig. 3.

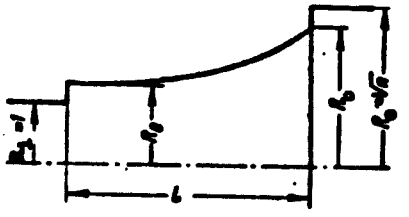

Fig. 4.

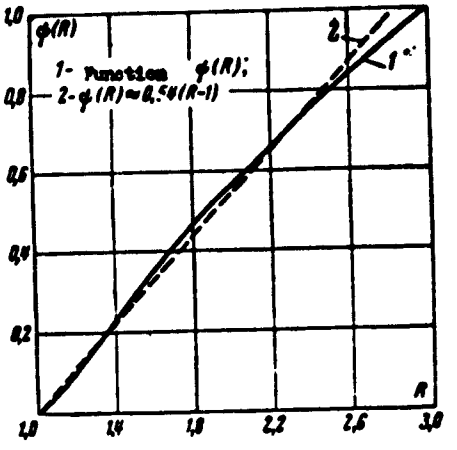
φ(R)
1- Function φ(R);
2- φ(R)≈0,54(R-1)
1,0
0,8
0,6
0,4
0,2
1,0
1,4
1,8
2,2
2,6
3,0
R
2
1

Fig. 5.

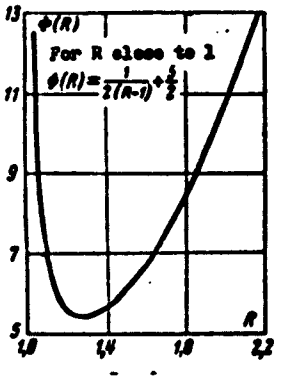
φ(R)
For R close to 1
φ(R)=1/2(R-1)+5/2
13
11
9
7
5
1,0
1,4
1,8
2,2
R

Fig. 6.

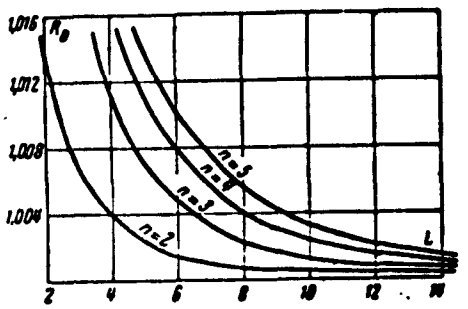
1,016
R_0
1,012
1,008
1,004
n=5
n=4
n=3
n=2
L
2
4
6
8
10
12
14

Fig. 7.

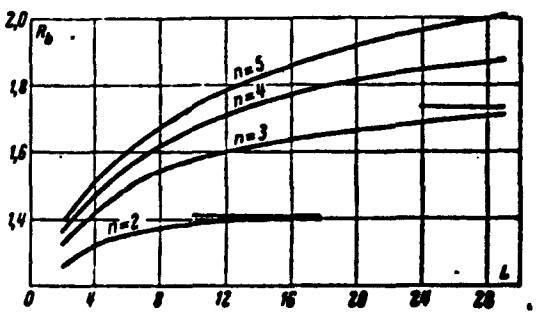
2,0
R_0
1,8
1,6
1,4
n=5
n=4
n=3
n=2
L
0
4
8
12
16
20
24
28

Fig. 8.

expansion angle determined by Formula (3). Differentiating Eq. (2) taking (1) into consideration we will find that expansion losses in this region amount to the following (more detail in Dorfman et al. [4]):

$$d\Delta_{exp} = \varphi(w - w_1)\,dw. \qquad (4)$$

where factor φ is determined by the value of the local expansion angle. The stream discontinuity equation for an axisymmetrical diffuser may be presented in the form:

$$\frac{w}{w_1} = \frac{F_1}{F} = \left(\frac{R_1}{R}\right)^2. \qquad (5)$$

We refer all the variables having length to the radius of the entry section of the diffuser:

$$\bar{R} = \frac{R}{R_1};\ \bar{x} = \frac{x}{R_1};\ \bar{L} = \frac{L}{R_1}.$$

In the following we will drop the strokes above the dimensionless magnitudes.

From (4) and (5) it follows that

$$d\Delta_{exp} = \frac{\rho w_1^2}{2}\,\varphi\left(1 - \frac{1}{R^4}\right)4\frac{dR}{R^5}.$$

Therefore loss factor $\zeta = \frac{\Delta_{exp}}{\frac{1}{2}\rho w_1^2}$ will be computed according to the formula

$$\zeta = 4\int_0^L \varphi(R)R\frac{R^2-1}{R^5}\,dx. \qquad (6)$$

Thus, the problem of finding the optimum diffuser shape reduces to finding a curve $R = R(x)$ such that, when integrating along it, integral (6) will assume its minimum value, i.e., towards the variational problem.

It is well known (e.g., cp. Lavrent'ev and Lyusternik [5]) that the integral

$$I = \int_a^b f(x, y, y')\,dx \qquad (7)$$

assumes its extreme value on the $y = y(x)$ curve on condition that

$$(d/dx) f'_{y'} - f'_{y} = 0 \text{ (Euler's equation)},$$

where f'_y and $f'_{y'}$ are partial derivatives in respect to y and y' from the integrand f.

If the integrand in (7) does not depend on x, the Euler's equation is integrated once and assumes the form

$$f(y, y') - f' f'_{y'}(y, y') = C,$$

where C is the integration constant.

Applying this condition to Expression (6) we easily obtain

$$[(R^2 - 1)/R^5] F(R') = C,$$

where the designations are that $F(R') = (R')^2 \varphi(R')$ and $\varphi'(R')$ is the derivative of the function of φ given by the graph in Fig. 1 in respect to $R' = \tan \theta/2$.

To solve Eq. (8) it is necessary to figure out $F(R')$ in advance. Since function $\varphi(R')$ is prescribed by the graph, the values of derivative $\varphi'(R')$ needed to compute $F(R')$ are determined numerically with the five point formula

$$\varphi'(R') = \frac{1}{h}\left(\Delta\varphi - \frac{1}{2}\Delta^2\varphi + \frac{1}{3}\Delta^3\varphi - \frac{1}{4}\Delta^4\varphi + \frac{1}{5}\Delta^5\varphi\right),$$

where h is the range of values of R' and $\Delta\varphi$, $\Delta^2\varphi$, ... are respectively the first, second, etc. differences. The function $F(R')$ obtained from the computations is shown in Fig. 3.

A sufficient minimum condition for integral (7) is the fulfillment of the inequality $f_{y,y'} \geqslant 0$ along the extremal $y = y(x)$.

For Expression (6) this condition has the form:

$$\frac{4(R^2-1)}{R^5} \cdot \frac{1}{R} \frac{dF(R')}{dR'} > 0.$$

But seeing that $4\frac{R^2-1}{R^2}\frac{1}{R'} > 0$, fulfillment of the last condition is equivalent to fulfilling the inequality

$$\frac{dF(R)}{dR} > 0. \qquad (9)$$

Inequality (9) is fulfilled only on the ascending side of curve $F(R')$ (Fig. 3). On the descending side of curve $F(R')$ we have $\frac{dF(R')}{dR'} \leqslant 0$. Consequently, at values of $R' > R'_{max}$, where R'_{max} is a root of the equation

$$\frac{dF(R')}{dR'} = 0, \qquad (10)$$

no such smooth curve $R(x)$ exists along which integral (6) assumes a minimum value.

It is also easy to see that Eq. (8) may be solved beginning only at values of $R \geqslant R_0$, where the magnitude R_0 depends on the choice of arbitrary constant C entering Eq. (8). Actually, by rewriting Eq. (8) in the form

$$F(R) = C\frac{R^2}{R^2-1}. \qquad (8')$$

it is easy to satisfy oneself that when $R \to 1$ the right side of the resulting equation increases infinitely and the left side is always bounded (Fig. 3). Therefore with values of R sufficiently near to 1 Eq. (8') has no solution and consequently with the indicated values of R there is no smooth curve realizing the minimum of integral (6).

From what has been set forth it follows that in the class of smooth curves of $R(x)$ (to be differentiated) there is none which at the prescribed length and degree of expansion gives a diffuser wall profile with minimum expansion losses. In this connection it is natural to suppose that the diffuser wall profile with minimum losses

does not represent a smooth curve but forms on intake (small values of R) and on exit (large values of R) abrupt area changes (sudden expansion), as is shown in Fig. 4. In this case the expression for the loss factor will take the form:

$$\zeta = \left(1 - \frac{1}{R_0^2}\right)^2 + 4\int_0^L \varphi(R') R' \left(1 - \frac{1}{R^2}\right) \frac{dx}{R^3} + \frac{1}{R_s^4}\left(1 - \frac{R_s^2}{n}\right)^2. \qquad (11)$$

Here the first and last members represent losses in sudden expansion on entry and exit, respectively, referred to the kinetic energy of the stream on entering the diffuser (Fig. 4 shows values of R_0 and R_s). If the curve of $R = R(x)$ when $0 < x < L$ is so chosen that it realizes the minimum of integral

$$I = 4\int_0^L \varphi(R') R' \frac{R^2 - 1}{R^3} dx,$$

then coefficient ζ will be a function only of R_0 and R_s will be the ordinate of the points through which the extremal passes.

The values of R_0 and R_s must be chosen from the conditions in Lavrent'ev and Lyusternik [5]:

$$\frac{\partial \zeta}{\partial R_0} = 0; \quad \frac{\partial \zeta}{\partial R_s} = 0.$$

The application of these conditions to (11) gives:

$$\begin{aligned} &\varphi'(R_0') R_0' + \varphi(R_0') - 1 = 0; \\ &\varphi'(R_s') R_s' + \varphi(R_s') - \frac{n - R_s^2}{n(R_s^2 - 1)} = 0. \end{aligned} \qquad (12)$$

Function $F(R')$ on the left side of Eq. (8) may with sufficient accuracy be approximated by a power relation (Fig. 3) within the limits from $R' = 0$ to a value of R'_{max} determined by the solution to Eq. (10).

This function may be written, for example, in the form

$$F(R') = 51 (R')^{3.5}.$$

Then Euler's equation for the indicated values of R' will have the form:

$$51(R')^{2.5} = C\frac{R^5}{R^5-1}. \qquad (13)$$

Hence after integration and slight transformations we obtain

$$x = \left(\frac{51}{C}\right)^{0.286}[\psi(R) - \psi(R_0)], \qquad (14)$$

where

$$\psi(R) = \int_0^R \left(\frac{R^5-1}{R^5}\right)^{0.286} dR.$$

Figure 5 shows function $\psi(R)$.

If we exclude the constant C from Eq. (14) (C can be determined by setting x = L and R = R_s in the equation), we will have:

$$\frac{x}{L} = \frac{\psi(R) - \psi(R_0)}{\psi(R_s) - \psi(R_0)}. \qquad (15)$$

The tangent of the slope angle R' may be determined from Eq. (13) by first substituting in it the value of the constant:

$$R' = \left(\frac{R^5}{R^5-1}\right)^{0.286} \cdot \frac{\psi(R_s) - \psi(R_0)}{L}. \qquad (16)$$

Equations (15) and (16) determine the form of the diffuser having minimum expansion losses.

In order that these equations may be used, the method of determining the magnitudes of R_0 and R_s must be indicated. Let us write Eq. (16) for the beginning and end of the diffuser:

$$\left.\begin{aligned} R_0' &= \left(\frac{R_0^5}{R_0^5-1}\right)^{0.286} \cdot \frac{\psi(R_s) - \psi(R_0)}{L}; \\ R_s' &= \left(\frac{R_s^5}{R_s^5-1}\right)^{0.286} \cdot \frac{\psi(R_s) - \psi(R_0)}{L}. \end{aligned}\right\} \qquad (17)$$

If we adduce Eq. (12), introduce the designations

$$\Phi(R) = \frac{R^5}{R^5-1}; \quad A(R') = \varphi'(R')R' + \varphi(R')$$

and divide the first of Eqs. (17) by the second, then the system

(12), (17) may be written in the form

$$A(R'_0) = 1;$$

$$A(R'_s) = \frac{n - R_s^2}{n(R_s^2 - 1)};$$

$$\frac{R'_0}{R'_s} = \left[\frac{\Phi(R_0)}{\Phi(R_s)}\right]^{0.286};$$

$$R'_0 = [\Phi(R_0)]^{0.286} \cdot \frac{\psi(R_s) - \psi(R_0)}{L}. \qquad (18)$$

The graphs of the functions $\Phi(R)$ and $A(R')$ are shown in Figures 6 and 3, respectively. From the first equation we easily find that $R'_0 = 0.177$. Further, for each pair of values $\underline{n}$ and R_s from the second equation we find R'_s, and then from the third and fourth, the corresponding values of R_0 and L. From the data obtained we construct the relations $R_0 = f_1(L)$ and $R_s = f_2(L)$ for several values of $\underline{n}$ (Figs. 7 and 8). Let us remember that the magnitudes R_0, R_s, and L refer to radius R_1 of the entry section of the diffuser.

From Figure 7 it follows that the value of R_0 for the usually used diffusers is practically no different from unity. This means that the sudden expansion on entry is slight and can be neglected. As for the sudden expansion on exit, that is very considerable at small lengths (Fig. 8) tends to zero when L increases, so that each curve of $R_s = f_2(L)$ has a horizontal asymptote $R_s = \sqrt{n}$. From Fig.8 it also follows that at a given dimensionless length the role of sudden expansion increases with the increase in $\underline{n}$.

Optimum diffuser shape, as was shown above, is in the part where there is no abrupt expansion determined by Eqs. (15) and (16). Notwithstanding that the local expansion angle determined by Eq. (16) is a variable magnitude, function $R(x)$ is close to the linear. Actually, the nature of function $R(x)$ is determined by the form of function $\psi(R)$ which differs very slightly from the linear (Fig. 5):

$$\psi(R) \approx 0.84(R - 1).$$

Thus the optimum is a stepped diffuser consisting of a part little different from the conical with a degree of expansion of R_s^2 and abrupt expansion on exit.

The work of Idel'chik [2] shows the result of an experimental comparison of flat diffusers of various shapes*. Of the three diffusers, isograde, rectilinear (θ = const), and stepped, with the same length and degree of expansion, the best proved to be the stepped one. The same work displays a systematic investigation of flat isograde and rectilinear diffusers. A comparison of the efficiency of these diffusers shows that at small equivalent expansion angles

$$\tan\frac{\theta_{eq}}{2} = \frac{\sqrt{n}-1}{L}$$

losses in the rectilinear diffuser are found to be less than in the isograde. With substantial equivalent angles the isograde diffuser proves to be more efficient. These conclusions agree with the results of this work. Actually, at small equivalent angles (small values of n and large ones of L) the role of abrupt expansion at the exit of an optimum diffuser, as follows from Fig. 8, is small; and therefore the rectilinear diffuser is nearer the optimum than the isograde is. Contrariwise, with large values of θ_{eq} (large n and small L) abrupt expansion on exit from the optimum diffuser is found to be substantial and consequently in this case the isograde diffuser will be nearer the optimum than the rectilinear.

In conclusion, let us note that in the examined problem only expansion losses were taken into consideration. It is easy,

*Unfortunately, similar data for axisymmetrical diffusers are lacking in the literature known to us.

however, to show that allowance for friction losses, which in the majority of cases are small in comparison with expansion losses, does not practically change the results.

Conclusions

The variational problem of the shape of a diffuser with minimum losses has been examined in this work.

We have shown that the optimum is a diffuser consisting of a part close to the conical and an abrupt expansion on exit.

The results we obtained agree qualitatively with the published experimental data on flat diffusers.

REFERENCES

1. B. N. Yur'ev. Experimental Aerodynamics. Oborongiz, 1939.

2. I. Ye. Idel'chik. Promyshlennaya Aerodinamika, No. 3, 1947.

3. G. N. Abramovich. Applied Gas Dynamics. Gostekhizdat, 1953.

4. A. Sh. Dorfman, M. M. Nazarchuk, N. I. Pol'skiy and M. I. Saykovskiy. Aerodynamics of Diffusers and Exhaust Pipes of Turbine Engines. Izd. AN USSR, 1960.

5. M. A. Lavrent'ev and L. A. Lyusternik. A Course in Variational Calculus. Gostekhizdat, 1950.

NOMOGRAMS FOR THE APPROXIMATE CALCULATION OF PROFILE FLOW IN TURBINE GRILLS

G. Ya. Shnitser

A. N. Sherstyuk [1] has proposed an approximate method of calculating the distribution of velocities on the profile perimeter of turbine grid vanes based on simple solutions for the flow of an incompressible fluid in curvilinear channels. To compute velocity w_1 at point A on the back of a vane (Fig. 1) Sherstyuk proposes using the following formula after having inscribed in the inter-vane channel a circle touching the vanes at A and B and after having determined the width of the channel along the equipotential line AB:

$$\overline{w}_1 = \overline{t} \cdot \frac{\frac{1}{\overline{h}}}{\frac{1}{1+0{,}29\overline{h}} - \frac{\overline{h}}{2(2+\overline{h})\cdot\overline{R}_2}}. \qquad (1)$$

where $\overline{w}_1 = w_1/W_z$; $\overline{R}_2 = R_2/R_1$; $\overline{h} = h/R_1$; $\overline{t} = t/R_1$; w_1 is the stream velocity on the back of the vane at point A; w_z, the expenditure component of velocity; R_2, the radius of curvature of the concave side of the vane; R_1, the radius of curvature of the back of the vane; $\underline{h}$, the width of the channel measured along the equipotential line.

Stream velocity w_2 on the concave side of the vane is computed from this formula:

$$\frac{\bar{w}_2}{\bar{w}_1} = \frac{1 - 0{,}5\frac{\bar{h}}{\bar{R}_2}}{1 + 0{,}5\bar{h}}. \qquad (2)$$

Despite the fact that two works [2, 3] later proposed somewhat more accurate formulas for computing flow in curvilinear channels, Sherstyuk's method is widely used also at the present time for designing turbine vanes because of its simplicity and sufficient accuracy for qualitative estimates. It is especially useful in cases where it is requisite quickly to calculate the nature of the profile to be used and also for obtaining a first approximation for more rigorous calculations.

Therefore it is of interest for shortening the computations to determine stream velocities from the nomograms proposed below instead of from Formulas (1) and (2).

Let us rewrite Formula (1) in the form

$$\bar{w}_1 = \bar{T}_1 \cdot F_1, \qquad (3)$$

where

$$F_1 = \frac{\frac{1}{\bar{h}}}{\frac{1}{1 + 0{,}29\bar{h}} - \frac{\bar{h}}{2(2+\bar{h})\bar{R}_2}}. \qquad (4)$$

Instead of (4) we may write

$$\left[\frac{1}{F_1}\right]\left[-\frac{1 + 0{,}29\bar{h}}{\bar{h}}\right] + \left[\frac{1}{\bar{R}_2}\right]\cdot\left[-\frac{1 + 0{,}29\bar{h}}{2(2+\bar{h})}\cdot\bar{h}\right] + 1 = 0. \qquad (5)$$

The last expression is an equation of the fourth nomographic order (in the Cauchy form) in respect to the expressions in brackets. Such equations may be represented in the form of nomograms of aligned

points.

On the basis of our experience with the calculations we will assume the following limits of change in the variables in Eq. (5):

$$\left.\begin{array}{l} 1 \leqslant \bar{R}_2 \leqslant 5; \\ 0{,}2 < \bar{h} < 2. \end{array}\right\} \qquad (6)$$

In addition, the following may be encountered:

$$\left.\begin{array}{l} \bar{R}_2 = \infty; \\ 0 < \bar{h} < 0{,}2. \end{array}\right\} \qquad (7)$$

In this case it is more convenient to use Formulas (1) and (2) which are considerably simplified and take on the form

$$\bar{w}_1 = \bar{\tau}\left[\frac{1}{\bar{h}} + 0{,}29\right]; \qquad (8)$$

$$\bar{w}_2 = \bar{w}_1\left[\frac{1}{1 + 0{,}5\bar{h}}\right]. \qquad (9)$$

The nomogram of Eq. (5) for computing the value of F_1 with respect to $\bar{R}_2$ and $\bar{h}$ consists of the rectilinear scales $\bar{R}_2$ and F_1 intersecting each other at a right angle and a curvilinear scale $\bar{h}_1$. The scale markings corresponding to the values of $\bar{R}_2$, $\bar{h}$, and F_1 connected by Formula (4) lie on a straight line (Fig. 2). The scales of $\bar{R}_2$ and F_1 are isometric.

The curve on which scale $\bar{h}_1$ is located is constructed from equations

$$\left.\begin{array}{l} x = \frac{1}{\bar{h}} + 0{,}29; \\ y = \left[\frac{1}{\bar{h}} + 0{,}29\right]\frac{\bar{h}}{2(2 + \bar{h})}. \end{array}\right\} \qquad (10)$$

The value of $\bar{h}$ changes from 0.2 to 2.0; $\underline{x}$ is plotted along axis F_1 and $\underline{y}$ along axis $\bar{R}_2$ in the units of those scales. At points $\underline{x}$, $\underline{y}$ on curve $\bar{h}_1$ are inscribed the values of $\bar{h}$ at which these points were computed.

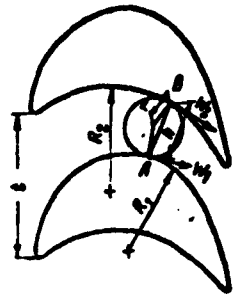

Fig. 1.

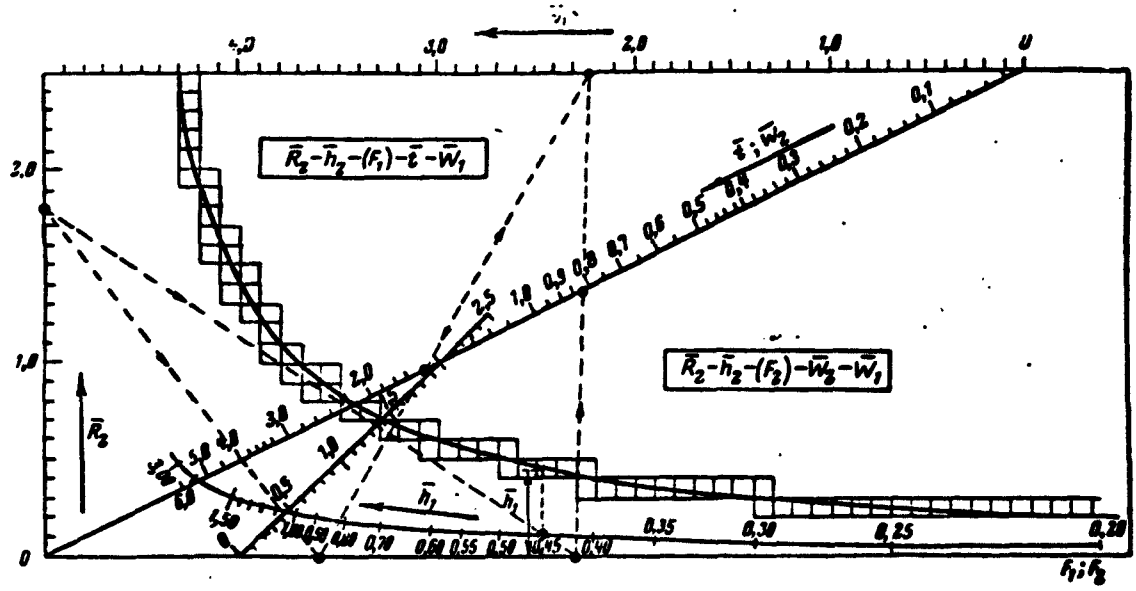
$\bar{R}_2-\bar{h}_2-(F_1)-\bar{c}-\bar{W}_1$
$\bar{R}_2-\bar{h}_2-(F_2)-\bar{W}_2-\bar{W}_1$
$\bar{R}_2$
$\bar{h}_1$
$\bar{c}; \bar{W}_2$
$f_1; f_2$

Fig. 2.

The construction of the $\bar{h}_1$ scale will be simplified if we use the hyperbolic function $\underline{x} = (1/\bar{h}) + 0.29$. By constructing the graph of this auxiliary hyperbola it is easy to determine the value of $\bar{h}$ for any point on curve $\bar{h}_1$ as the ordinate of the hyperbola above this point (Fig. 2). Thus, on the $\bar{h}_1$ scale it is sufficient to write down only basic reference points (0.2, 0.3, 0.4, etc.).

After the value of F_1 has been found, velocity $\bar{w}_1$ is determined from Eq. (3) or, more conveniently from the z-nomogram corresponding to this equation. The z-nomogram consists of the parallel rectilinear scales F_1 and $\bar{w}_1$ and the rectilinear scale $\bar{t}$ intersecting them. The F_1 and $\bar{w}_1$ scales coincide with the F_1 and $\bar{R}_2$ scales of the preceding nomogram. The $\bar{t}$ scale is projective and is plotted directly from the equation $\bar{t} = \bar{w}_1/F_1$. The scale markings corresponding to the values of F_1, $\bar{t}$, $\bar{w}_1$ are connected by Formula (3) and lie on a straight line. For convenience in use both nomograms are combined so that their F_1 scales coincide and may be blank.

In order to design nomograms for calculating the velocity on the concave side of the vane we rewrite Formula (2) in the form

$$\bar{w}_1 = \bar{w}_2 \cdot F_2. \tag{11}$$

where

$$F_2 = \frac{1 + 0{,}5\bar{h}}{1 - 0{,}5\frac{\bar{h}}{\bar{R}_2}}. \tag{12}$$

Instead of (12) we may write

$$\left[\frac{1}{F_2}\right]\cdot[-1] + \left[-\frac{\bar{h}}{2+\bar{h}}\right]\left[1 + \frac{1}{\bar{R}_2}\right] + 1 = 0. \tag{13}$$

Equation (13) may be in the form of a nomogram of aligned points with two intersecting scales. The third scale in this case will also be rectilinear and isometric. It is constructed according

to the equations

$$x=\frac{\bar{h}}{2};\ y=\frac{\bar{h}}{2}+1. \qquad (14)$$

As before also, $\underline{x}$ is plotted along the F_2 axis and $\underline{y}$ along the R_2 axis in units of these scales.

The rule for using the nomogram is evident from Fig. 2. After the value of F_2 has been found, velocity $\bar{w}_2$ is determined by Eq. (11) or, more conveniently, from the z-nomogram. In the latter case the already mentioned z-nomogram is used for figuring $\bar{w}_1$ with only this difference, that instead of F_1 the value of F_2 is plotted on that scale, and the value $\bar{w}_2$ instead of $\bar{t}$. Thus, all the nomograms described above are combined (Fig. 2). They may easily be constructed since almost all the scales are isometric. The nomograms guarantee velocity computations to an accuracy of three significant digits; greater accuracy is superfluous, as the initial value of $\underline{h}$ in this calculation is taken from a drawing with the same accuracy.

An example of computation:

From the drawing are taken the following data: $\bar{R}_2 = 1.78$, $\bar{h} = 0.45$, $\bar{t} = 0.83$.

Determining velocity $\bar{w}_1$. Key: $\bar{R}_2 - \bar{h}_1 - (F_1) - \bar{t} - \bar{w}_1$.

We join point 1.78 on scale $\bar{R}_2$ with point 0.45 on scale $\bar{h}_1$ with a straight line which we extend to intersect with the F scale. Between the point thus obtained and point 0.83 on scale $\bar{t}$ we draw a staight line at whose intersection with the $\bar{w}_1$ scale we read the answer $\bar{w}_1 = 2.22$.

Determining velocity $\bar{w}_2$. Key: $\bar{R}_2 - h_2 - (F_2) - \bar{w}_2 - \bar{w}_1$.

Point 1.78 on vertical scale $\bar{R}_2$ and point 0.45 on scale $\bar{h}_2$ are connected by a straight line projected to intersect scale F.

Through the point thus obtained and point 2.22 on scale $\bar{w}_1$ we draw a straight line at whose intersection with scale $\bar{w}_2$ we read the answer – $\bar{w}_2 = 1.58$.

REFERENCES

1. A. N. Sherstyuk. Teploenergetika, No. 8, 1955.

2. G. S. Samoylovich and A. N. Sherstyuk. Izvestiya AN SSSR, No. 4, 1958.

3. M. I. Zhukovskiy. Calculating the Flow past Grid Vanes in Turbine Engines. Mashgriz, 1960.

DISTRIBUTION LIST

DEPARTMENT OF DEFENSE	Nr. Copies
HEADQUARTERS USAF	
AFCIN-3D2	1
ARL (ARB)	1
OTHER AGENCIES	
CIA	1
NSA	6
DIA	9
AID	2
OTS	2
AEC	2
PWS	1
NASA	1
ARMY	3
NAVY	3
RAND	1

MAJOR AIR COMMANDS	Nr. Copies
AFSC	
SCFDD	1
ASTIA	25
TDETL	5
TDEDP	5
SSD (SSF)	2
BSD (BSF)	1
AFFTC (FTY)	1
AFSWC (SWF)	1